electronics

MDPI

Article

Evaluation of the Effectiveness of Protecting Three-Dimensional Printers against Acoustic Infiltration

Andrzej Stańczak and Ireneusz Kubiak *

Electromagnetic Compatibility Department, Military Communication Institute—National Research Institute, Warszawska 22A Str., 05-130 Zegrze Poludniowe, Poland; a.stanczak@wil.waw.pl
* Correspondence: i.kubiak@wil.waw.pl

Abstract: Three-dimensional printers are increasingly used in design work when designers want to quickly and inexpensively verify their solutions. However, based on the sounds made by the printer during its operation, it is possible to determine the shape of the printed object with quite high accuracy. The above fact should be taken into account if information about this object needs to be protected. The article presents a way to protect a 3D (Three-Dimensional) printer against acoustic infiltration. The research study was carried out using the Zortrax M200 Plus printer for LPD (Layer Plastic Deposition) technology, which is an equivalent of the popular FDM/FFT (Fused Deposition Modeling/Fused Filament Fabrication) 3D printing technology using thermoplastic. The frequencies of acoustic signals related to the operation of stepper motors and the printing platform were identified. These signals enable the reconstruction of the shape of printed objects. It was examined whether the appropriate type and required level of masking noise can be selected for a given type of printer in order to protect it against acoustic infiltration. The masking properties of selected color noises were compared with those of white noise and the optimal intensity levels were determined at which the acoustic safety of the tested printer can be ensured. It was underlined that the research results refer only to the tested printer and should not be generalized to other types of 3D printers.

Keywords: 3D printer; additive manufacturing; acoustic signal; infiltration; color noise; data acquisition; spectrogram

check for updates

Citation: Stańczak, A.; Kubiak, I. Evaluation of the Effectiveness of Protecting Three-Dimensional Printers against Acoustic Infiltration. *Electronics* **2023**, *12*, 4641. https://doi.org/10.3390/electronics12224641

Academic Editor: Juan M. Corchado

Received: 16 October 2023
Revised: 8 November 2023
Accepted: 10 November 2023
Published: 14 November 2023

Copyright: © 2023 by the authors. Licensee MDPI, Basel, Switzerland. This article is an open access article distributed under the terms and conditions of the Creative Commons Attribution (CC BY) license (https://creativecommons.org/licenses/by/4.0/).

1. Introduction

Three-dimensional printing is a complex definition for many technologies that differ in manufacturing processes, materials used and the type of objects that can be made from them. Based on the literature analysis, the main 3D printing technologies can be characterized as follows:

- FDM (Fused Deposition Modeling)/FFF (Fused Filament Fabrication)—3D printing from thermoplastics. This is the most popular technology on the home and semi-professional printer market. The printing material is plastic in the form of a monofilament. This monofilament is heated to the appropriate temperature during the 3D printing process. After obtaining a semi-liquid consistency, the monofilament is put on layer by layer (as a result of the printing platform moving down or by moving the printing head up) using the printing head. Bonding occurs under the influence of temperature. FDM printers can use materials such as ABS or PLA. The operation of the printer is based on the working of three stepper motors, which are the source of sound signals.
- SLA (stereolithography)—3D printing from resins hardened with a laser beam. This technology uses a resin hardened under the influence of light as a printing material. The semi-liquid resin is located in a special container in which the work table is placed. The material hardens during the action of the laser beam. The table with resin is lowered by one layer and the beam reproduces the desired shape in the XY plane.

- DLP (Digital Light Processing)—3D printing from resins hardened with a projector beam. In this technology, the resin is hardened by the light of the projector, which is placed under the resin container. The entire layer is hardened at once.
- PolyJet/MJP (PolyJet/Multi-Jet Printing)—3D printing from resins hardened with UV light. Printing is conducted in a similar way to printing on paper using a laser or ink. The print head moving over the platform (work table) sprays a layer which is at the same time hardened by ultraviolet radiation.
- CJP (Color Jet Printing)—3D printing from gypsum powders in full color. A layer of powder is placed on the surface of the work table, and the printer head sprays colored ink and binder in appropriate places. The print is chemically hardened [1,2].
- Binder Jetting—3D printing from powdered metal, ceramic, or sand. This printing technology does not require the use of supporting structures. The process of creating objects resembles traditional inkjet printing. The Binder Jetting method is used in industry to create, for example, foundry molds [3].
- SLS (Selective Laser Sintering)—3D printing from powdered plastics selectively glued and welded using a laser beam [3].
- SLM/DMLS (Selective Laser Melting/Direct Metal Laser Melting)—3D printing from powdered metals melted using a laser beam.
- EBM (Electron Beam Melting)—3D printing from powdered metals melted using an electron beam.
- MJF (Multi-Jet Fusion)—3D printing from powdered polyamide, which is selectively glued and welded at a high temperature.
- LOM (Laminated Object Manufacturing)—3D printing using layers of paper with glue and polyester laminate cut using a laser.
- Bioprinting—3D printing from living biological material. In this way, fragments or even entire organs can be obtained [3].

The abovementioned 3D printing technologies use different printing materials and different methods of hardening them. The article further focuses on the analysis and possibilities of masking sound signals correlated with printed shapes for the Zortrax M200 Plus printer, which uses FDM technology and PLA printing material. The choice of the printer resulted from its popularity and availability.

Three-dimensional printers use additive manufacturing (AM) and they are often applied in many design offices and enterprises. The unquestionable advantages of additive printing include rapid product prototyping before the commercialization stage and easy correction of any design errors before production implementation [4,5]. Particular interest in this technology can be observed in the automotive, aviation, arms and biomedical industries. In many cases, 3D printers are used to illustrate new ideas in the form of models that should be kept secret until official presentation. As with other IT devices, 3D printers are also a potential object of physical and cyberattacks [6,7]. As is known, these printers produce emissions E during their operation in side-channel attacks [8–18]: acoustic $E_{acoustic}$, vibration $E_{vibration}$, electromagnetic E_{em}, power E_{power} and thermal $E_{thermal}$, which have features correlated with the printed object. The emissions can be used in the process of obtaining information about the shape of this object non-invasively. This may result in premature disclosure of project results [19–23]. The article focuses on issues related to the acoustic emission of printers ($E_{acoustic}$) in the side channel. This issue has been discussed, among others, in [8,10,14,24]. Various possibilities for improving the safety of printers against acoustic infiltration were presented, but none of the solutions indicated a method involving the use of color noise masking.

In [8], an innovative acoustic side-channel attack model for FDM technology was presented. The shape of the printed object (a key) was reproduced with quite high accuracy. It was found that to improve protection against acoustic infiltration and to make G-code that controls the operation of a printer, making the reconstruction process more difficult, randomness of the motor movement could be introduced into this code. However, the disadvantage of such a countermeasure will be the delay in the overall printing time.

In [10], the selected 3D printer with the ME3DP (Material Extrusion 3D Printing) technology was tested to analyze the existing risk. Simple objects were printed during its operation to identify the stepping motor operations that are emission sources in the secondary channels. The carried-out analyses were focused on finding the correlation between the registered emissions and the printer head (printhead) movements when printing an object. It was shown that the analysis of the registered sensitive signal runtimes and their spectrograms allows us to recreate the printed object's shape. The studies focused on measuring the acoustic signals that came from the stepping motors. The analysis of the possibilities of identifying the shapes of printed objects was based on the visual method.

In [14], it was pointed out that most of the research works were focused on protecting the intellectual property (IP) of the product after it had been built. However, there is a presence of a persistent threat to the confidentiality of the product during the manufacturing process. Additive manufacturing is based on the tight integration of the cyber and physical domains. One of the challenges is preventing confidentiality breach due to physical-to-cyber domain attacks, where hackers can analyze various analog emissions from the side channels to steal the cyber-domain information. This information theft is based on the assumption that the attacker can estimate the relationship between analog emissions (acoustics, power, electromagnetic, etc.) and the cyber-domain data (such as G-code). Therefore, a solution incorporated into computer-aided manufacturing tools was proposed, such as the *slicing algorithm* and *tool-path planning* which are in the cyber domain. This novel methodology provides the physics- and data-driven leakage models for acoustic side channels, defines various design variables (orientation and speed), provides an optimization algorithm and incorporates it in the digital process chain. For various reference 3D models, an average reduction in mutual information of approximately 25% was achieved.

The problem of acoustic emissions from dot-matrix printers was also considered [24]. An attack was presented that allowed for the reconstruction of the text of prescriptions printed in English. In the experiments conducted, 72% of printed words were recovered, and even up to 95% if contextual knowledge of the text was assumed, with the microphone at a distance of 10 cm from the printer.

The sources of sensitive signals are primarily the printer's stepper motors, as well as the print head and platform, which are driven by these motors in the X and Y directions (head) and Z direction (platform) [25–27], as shown in Figure 1.

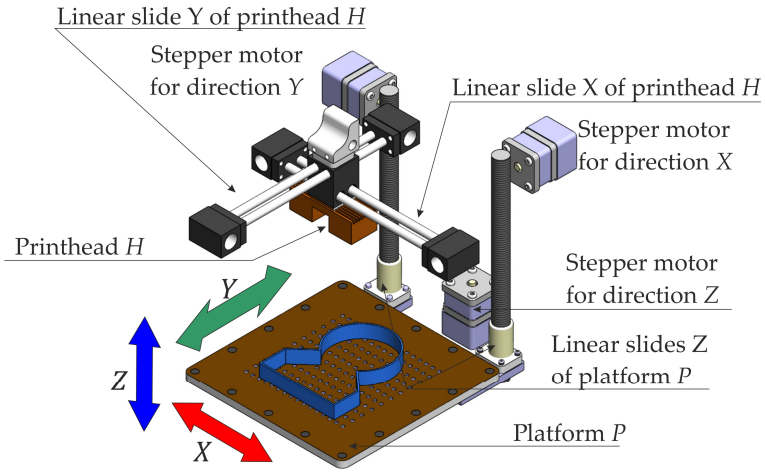


Figure 1. Basic mechanical elements of a 3D printer.

When printing confidential device components, protecting 3D printers against acoustic infiltration is a particularly important task because the $E_{acoustic}$ emissions of 3D printers can be easily captured. Based on the literature studies carried out, it can be concluded that the issue of effective security for this type of printer is not yet sufficiently recognized [28–30].

The aim of the research was to determine the required level of generated masking noise $L_{acoustic\_noise}$ which would prevent the reconstruction of information about the shapes

of printed objects based on the received acoustic emissions $E_{acoustic}$. Intuitively, we would expect that the level of masking noise should meet the relationship:

$$L_{acoustic\_noise} - L_{acoustic\_printer} = \Delta L > 0, \quad (1)$$

where:

$L_{acoustic\_printer}$—acoustic signal level of 3D printer;
$L_{acoustic\_noise}$—acoustic noise level masking acoustic signal of 3D printer.

The ΔL values, depending on the type of noise used, were determined on the basis of tests and analyses of spectrograms obtained for various levels of masking noise. Before starting the research, objects with various degrees of complexity were designed (the number of intersecting planes was equal from several to a dozen). The designs were made using the free Sketchup Make software v.17.2.2555, which is part of the commercial version of Sketchup Pro. The software enables the design of three-dimensional models. Many tools are available, such as shapes, lines, arcs, freehand drawing, as well as the ability to transform 2D drawings into 3D objects.

Figure 2 shows photographs of these objects after printing on the Zortrax M200 Plus printer, which was the subject of research by the authors of the article. The preliminary tests were repeated for each of the designed objects.



(**a**) (**b**)

Figure 2. Three-dimensional objects designed for research on securing a 3D printer against acoustic infiltration: (**a**) test set, (**b**) objects selected for research—the Lock and the Ghost.

It was decided to conduct the actual research on two selected objects of low and high complexity, called the Lock (gray color) and the Ghost (red color), respectively. Based on the obtained results of preliminary tests, it was found that regardless of the geometry of the objects (angles of inclination of diagonal lines, radii of arcs), the frequencies of signals containing important information about the printed object for tested printer are in the range from approximately 9 kHz up to approximately 20 kHz.

2. Methods

2.1. Characteristics of Noise in the Acoustic Band

It is generally considered that noise is an undesirable phenomenon, especially when its intensity is high. It appears in various forms: the noise of equipment operation, the noise of urban surroundings or part of the sounds of nature. In some cases, noise may be useful, for example, if it is used to mask sounds carrying sensitive information. As mentioned in Section 1, sounds generated during the operation of a 3D printer should be considered as such, because based on their analysis, the shape of the printed object can be reproduced with acceptable accuracy. The obvious conclusion seems to be that these "sensitive" sounds should be tried to be hidden by applying noise over them. Therefore, at the beginning of the research work, an analysis of the characteristics of various noises was carried out in terms of their masking features useful for a specific application.

Previous research [4] has shown that the sounds produced by the Zortrax M200 Plus printer, which may contain the most important information from the point of view of its infiltration susceptibility, are located in the frequency range f from approximately 9 kHz to approximately 19 kHz. Therefore, the selection of appropriate masking noise should take this fact into account.

The basic parameter determining the type of noise is the power spectral density $S(f)$. Depending on its characteristics, white noise and the so-called color noises are distinguished. The characteristics of popular noises in acoustics are given in Figure 3.

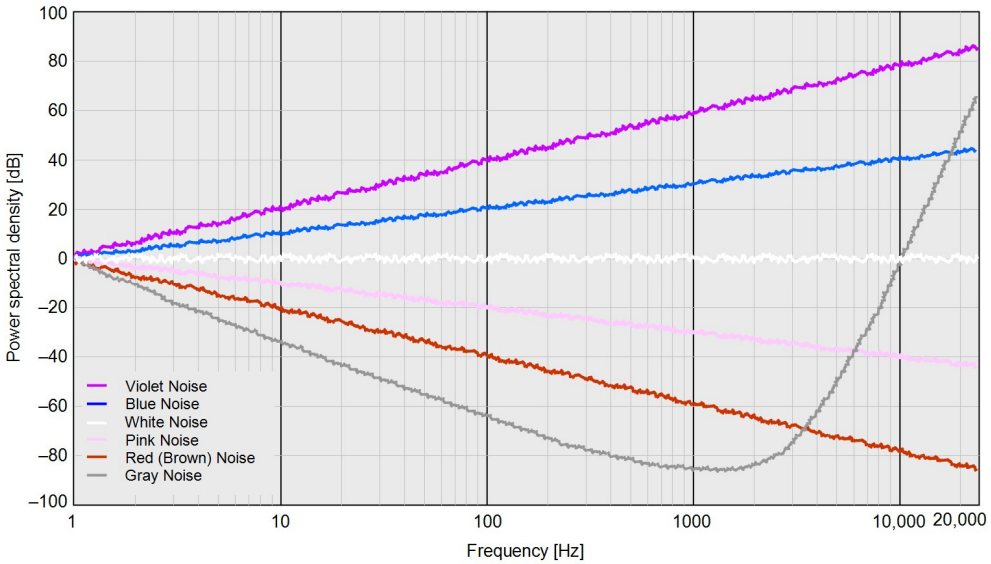


Figure 3. Distribution of power spectral density $S(f)$ as a function of frequency f for different noise colors (pink, red/brown, gray, white, blue, purple).

White noise is a type of sound with the spectral characteristics $S_W(f)$, where the sound pressure level for each frequency is approximately the same; the consequence of this is an increase in the sound level for increasingly higher octaves.

Red noise is characterized by a falling power spectrum $S_R(f)$ at a rate of 6 dB per octave (20 dB per decade). The power spectral density of this noise is inversely proportional to f^2. This noise was initially obtained by filtering white noise. Then, it was noticed that it could be produced using the so-called "random walk" or "drunkard's walk"—and by its similarity to the so-called Brownian movements, it was called "Brownian noise". In analogy to other colors of noise, over time, the name "brown noise" came to be used.

In practice, the noise generation method consists in obtaining another sample value by adding a small random number to the previous one, i.e., taking a random step length in a random direction. The spectrum of this noise is similar to the sound spectrum of an ocean or a large waterfall, due to the significant content of lower-frequency components.

Pink noise has intermediate properties between white and red noise (hence its name). The power spectral density $S_P(f)$ of this noise is directly proportional to $1/f$ and falls at a speed of 3 dB per octave (10 dB per decade). Pink noise can be easily obtained from white noise by passing it through an appropriate low-pass filter. It is worth adding that many natural phenomena produce noise similar to pink noise.

Blue noise is characterized by the fact that its spectral density $S_B(f)$ is directly proportional to f and grows at a rate of 3 dB per octave, which is the opposite of that of pink noise. Because this noise is dominated by higher-frequency components, it sounds like a hiss (completely devoid of bass). The name of the noise comes from optics because the color blue is at the higher end of the visible light frequency spectrum.

Violet noise, also called purple noise, is characterized by a power spectrum that increases by 6 dB per octave with increasing frequency (which is the opposite of red noise).

The power spectral density $S_V(f)$ of this noise is directly proportional to f^2. Purple noise is also called differential white noise because its samples are the result of calculating the differences of adjacent samples of the white noise signal ($\Delta x_t = x_t - x_{t-1}$). With regard to phenomena occurring in the natural environment, it can be said that the spectrum of violet noise is similar to the spectrum of the noise of boiling water.

Gray noise is white noise corrected according to a psychoacoustic curve of equal loudness. It is therefore noise that sounds equally loud for any arbitrarily cut equal section of the frequency band. From the acoustic point of view, it is like a "better" (in terms of human perception) version of white noise with a power spectral density of $S_G(f)$.

As a result of the analysis, it was found that the best features for masking the sounds of a working 3D printer should have three types of noise: blue, purple and gray. Therefore, sound samples of these noises were used for further laboratory tests, while white noise was used for comparison purposes. The aim of the research was to select the noise that has the best masking properties, at the lowest possible level of its intensity, and is acceptable to the staff operating the printer.

2.2. Test System

The proposed protection consists in masking the sounds produced by the printer during additive printing with appropriate noise. The effectiveness of this solution was tested in the system shown in Figure 4 (variant 1) and Figure 5 (variant 2). The system was placed in an anechoic chamber which allows researchers to separate additional sources of sounds.

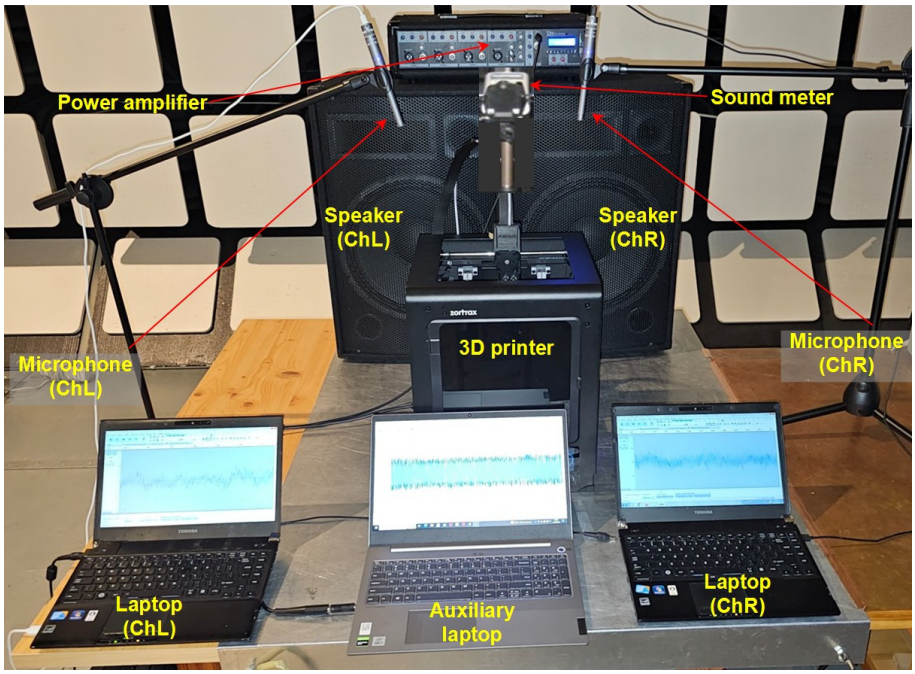


Figure 4. Test system—variant 1.

In variant 1, the Zortrax M200 Plus 3D printer was placed on a work table. At a distance of $R = 1$ m behind the printer, two Voice Kraft loudspeakers were placed, each with a power of $P_{max} = 300$ W ($P_{RMS} = 150$ W), efficiency of 94 dB (±3 dB), frequency response 30–20,000 Hz and impedance 8 Ω. These speakers were connected to the PDM-C405A Power Dynamics acoustic amplifier with an output power of $P = 800$ W ($P_{RMS} = 70$ W) and a frequency response of 50–20,000 Hz. A laptop was connected to the line input of the amplifier, on which "wav" files with selected types of noise were recorded. The noise intensity was measured using the Sound Level Meter TES 1350.

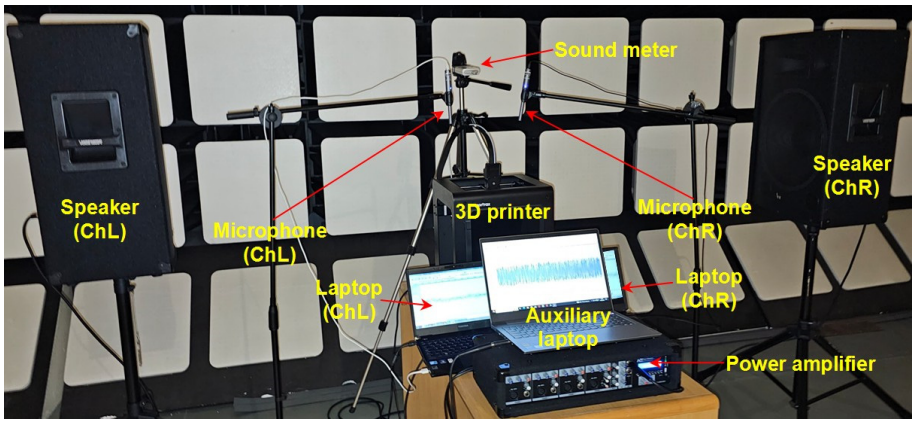


Figure 5. Test system—variant 2.

In variant 2, the speakers were mounted on stands placed on the side of the 3D printer, each at a distance of $R = 1$ m from the printer. In both variants, two UMIK-1 digital measurement microphones with a cardioid characteristic, with 48 kHz sampling and a frequency response of 20–20,000 Hz, were placed above the printer. Each microphone was mounted on a stand and connected to the USB port of the laptop recording the sounds of the right channel (ChR laptop) and left channel (ChL laptop), respectively.

Audacity applications were installed on ChR and ChL laptops, recording acoustic signals produced by the 3D printer during its operation. Each measurement session lasted approximately 60 s. The recording time was chosen so that the obtained spectrograms included at least several printing cycles of a given object, separated by head positioning phases (one cycle corresponded to printing one track).

Because, based on previously conducted simulation tests [31], it was not possible to determine measurable values of the $L_{acoustic\_noise}$ levels of the noise used (their regulation when generated in the Audacity software v.3.2.2 is dimensionless, with an available range from 0 to 1), the tests conducted in laboratory conditions were performed to enable the determination of these levels in decibels. This is important in the practical solution of protecting the printer against acoustic infiltration, due to the independence of the levels of recorded noise samples and the required acoustic noise level $L_{acoustic\_noise\ [\mathrm{dB}]}$ being determined only by adjusting the power amplifier.

3. Results and Discussion

3.1. Measurement of Acoustic Emissions from a 3D Printer When the Lock Object Was Printed

The Lock object is a solid consisting of six intersecting walls. Its horizontal section is shown in Figure 6. The printing process takes place in layers, and each layer consists of two paths: internal and external, marked in green and red in the drawing, respectively. The thickness of each track is approximately 0.6 mm. Characteristic points of the object where the direction of the print head movement changes are marked with letters A to F.

The print head performs the positioning phase (P1), positioning itself over point A. The printing phases are as follows (green lines in Figure 6):

A-B—a parallel line to the Y axis;
B-C—a diagonal line deviated from the Y axis by an angle of 45°;
C-D—$^{7}/_{8}$ circle with radius $r_1 = 2$ cm and a negative direction;
D-E—a diagonal line deviated from the X axis by an angle of −45°;
E-F—a parallel line to the Y axis;
F-A—a parallel line to the X axis.

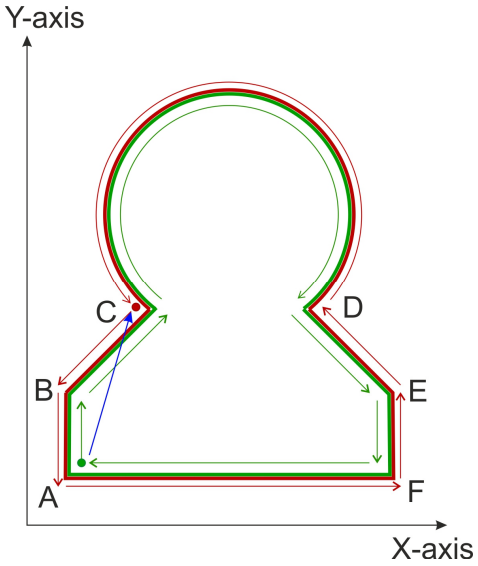


Figure 6. Horizontal cut of the Lock object (an external path—red color, an internal path—green color, a moving of the print head from the point A (after the printing internal path) to point C (to print the external path)).

After printing the internal path, the head performs the positioning phase (P2) for printing the external path: the platform moves down along the Z axis by approximately 2 mm, the head moves over the C point of the object and the platform moves up by approximately 1 mm. Then, the head continues printing the object in six returning phases (red lines in Figure 6):

C-*B*—a diagonal line deviated from the Y axis by an angle of 45°;
B-*A*—a parallel line to the Y axis;
A-*F*—a parallel line to the X axis;
F-*E*—a parallel line to the Y axis;
E-*D*—a diagonal line deviated from the X axis by an angle of −45°;
D-C$^{-7}/_{8}$ circle with radius $r_1 = 2$ cm and a negative direction.

After reaching point C, the platform moves down approximately 2 mm, the head is positioned above point A, then the platform moves up 1 mm and printing of the next layer begins.

Spectrograms of signals recorded during printing of the Lock object along with individual printing phases are shown in Figure 7.

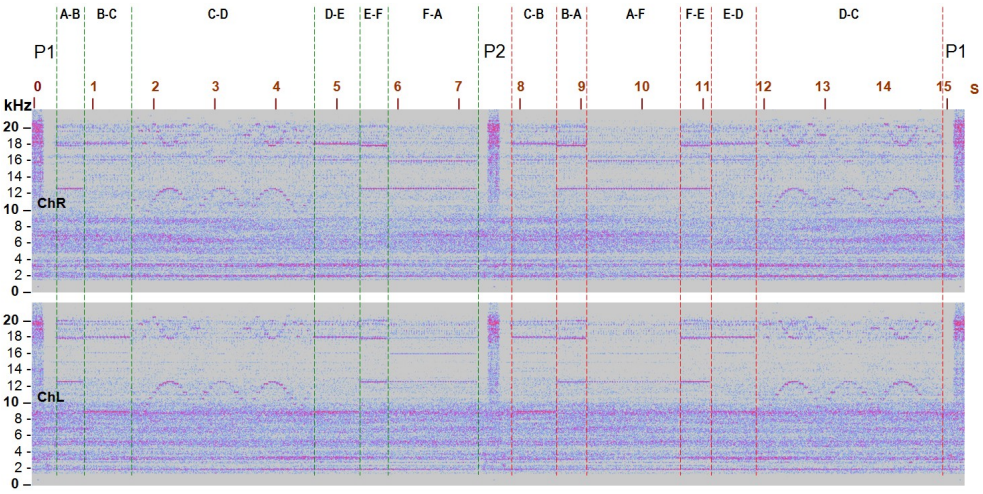


Figure 7. Spectrograms of 3D printer acoustic signals recorded during the printing of the Lock object.

3.2. Measurement of Acoustic Emissions from a 3D Printer When the Ghost Object Was Printed

The Ghost object is a solid consisting of fifteen intersecting walls. Its horizontal cut is shown in Figure 8.

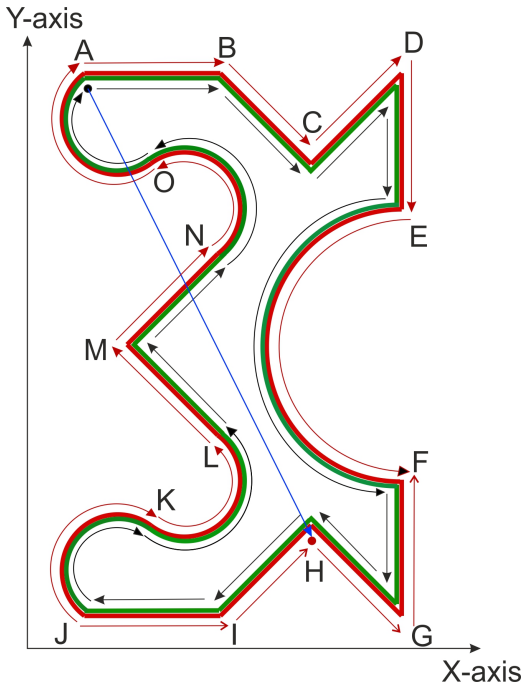


Figure 8. Horizontal cut of the Ghost object (an external path—red color, an internal path—green color, a moving of the print head from the point A (after the printing internal path) to point H (to print the external path)).

The printing process and its parameters were analogical to the Lock object. Characteristic points of the object where the direction of the print head movement changes are marked with letters A to O. The print head performs the positioning phase (P1), positioning itself over point A. The printing phases are as follows (green lines in Figure 8):

A-B—a parallel line to the X axis;
B-C—a diagonal line deviated from the X axis by an angle of $-45°$;
C-D—a diagonal line deviated from the X axis by an angle of $45°$;
D-E—a parallel line to the Y axis;
E-F—a semicircle with radius $r_1 = 2$ cm and a positive direction;
F-G—a parallel line to the Y axis;
G-H—a diagonal line deviated from the X axis by an angle of $-45°$;
H-I—a diagonal line deviated from the X axis by an angle of $45°$;
I-J—a parallel line to the X axis;
J-K—a semicircle with radius $r_2 = 1$ cm and a negative direction;
K-L—a semicircle with radius $r_2 = 1$ cm and a positive direction;
L-M—a diagonal line deviated from the X axis by an angle of $-45°$;
M-N—a diagonal line deviated from the X axis by an angle of $45°$;
N-O—a semicircle with radius $r_2 = 1$ cm and a positive direction;
O-A—a semicircle with radius $r_2 = 1$ cm and a negative direction.

After printing the internal path, the head performs the positioning phase (P2) for printing the external path: the platform moves down along the Z axis by approximately 2 mm, the head moves over the H point of the object and the platform moves up by approximately 1 mm. Then, the head continues printing the object—this time along the external path—in the following phases (red lines in Figure 8):

H-G—a diagonal line deviated from the X axis by an angle of $-45°$;

G-F—a parallel line to the Y axis;
F-E—a semicircle with radius $r_1 = 2$ cm and a negative direction;
E-D—a parallel line to the Y axis;
D-C—a diagonal line deviated from the X axis by an angle of $-45°$;
C-B—a diagonal line deviated from the X axis by an angle of $45°$;
B-A—a parallel line to the X axis;
A-O—a semicircle with radius $r_2 = 1$ cm and a positive direction;
O-N—a semicircle with radius $r_2 = 1$ cm and a negative direction;
N-M—a diagonal line deviated from the X axis by an angle of $45°$;
M-L—a diagonal line deviated from the X axis by an angle of $-45°$;
L-K—a semicircle with radius $r_2 = 1$ cm and a negative direction;
K-J—a semicircle with radius $r_2 = 1$ cm and a positive direction;
J-I—a parallel line to the X axis;
I-H—a diagonal line deviated from the X axis by an angle of $45°$.

Spectrograms of signals recorded during printing of the Ghost object (without noise masking) along with individual printing phases are shown in Figure 9.

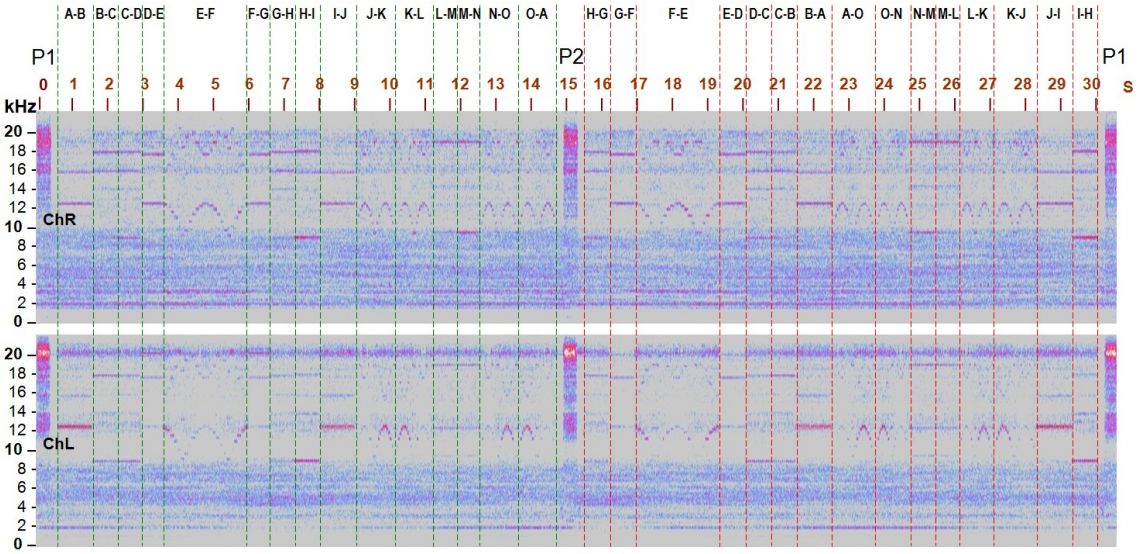


Figure 9. Spectrograms of 3D printer acoustic signals recorded during the printing of the Ghost object.

3.3. Testing the Effectiveness of Masking Acoustic Emissions of a 3D Printer Using Different Types of Noise

Comparing the spectrograms of 3D printer sound signals recorded during the printing of the Lock and the Ghost objects, it can be seen that the levels of revealing emissions do not depend significantly on the complexity of the printed object. Therefore, one representative object—the Ghost—was selected for further research on assessing the effectiveness of masking various types of noise.

In the printing of the selected object, white, blue, gray or purple noise at levels of 40 to 80 dB (with an interval of 10 dB) was used as a masking signal.

The spectrograms obtained from these measurements are presented in Figures 10–13, respectively.

Because the spectrograms obtained for the signals recorded in both channels were very similar, to improve the readability of the figures, only the spectrograms of the signals recorded in the right channel (ChR) are included.

White noise has quite good masking properties if its level is at least $L_{acoustic\_noise\_White} = 60$ dB. However, some image elements correlated with the printed Ghost object are identifiable. Therefore, the safe level of this noise from the point of view of ensuring information protection should be at least $L_{acoustic\_noise\_White} = 70$ dB. Increasing the white noise to

$L_{acoustic\_noise\_White} = 80$ dB masks the signal in the entire frequency range considered. At this level, even the print head positioning phases are not recognizable.

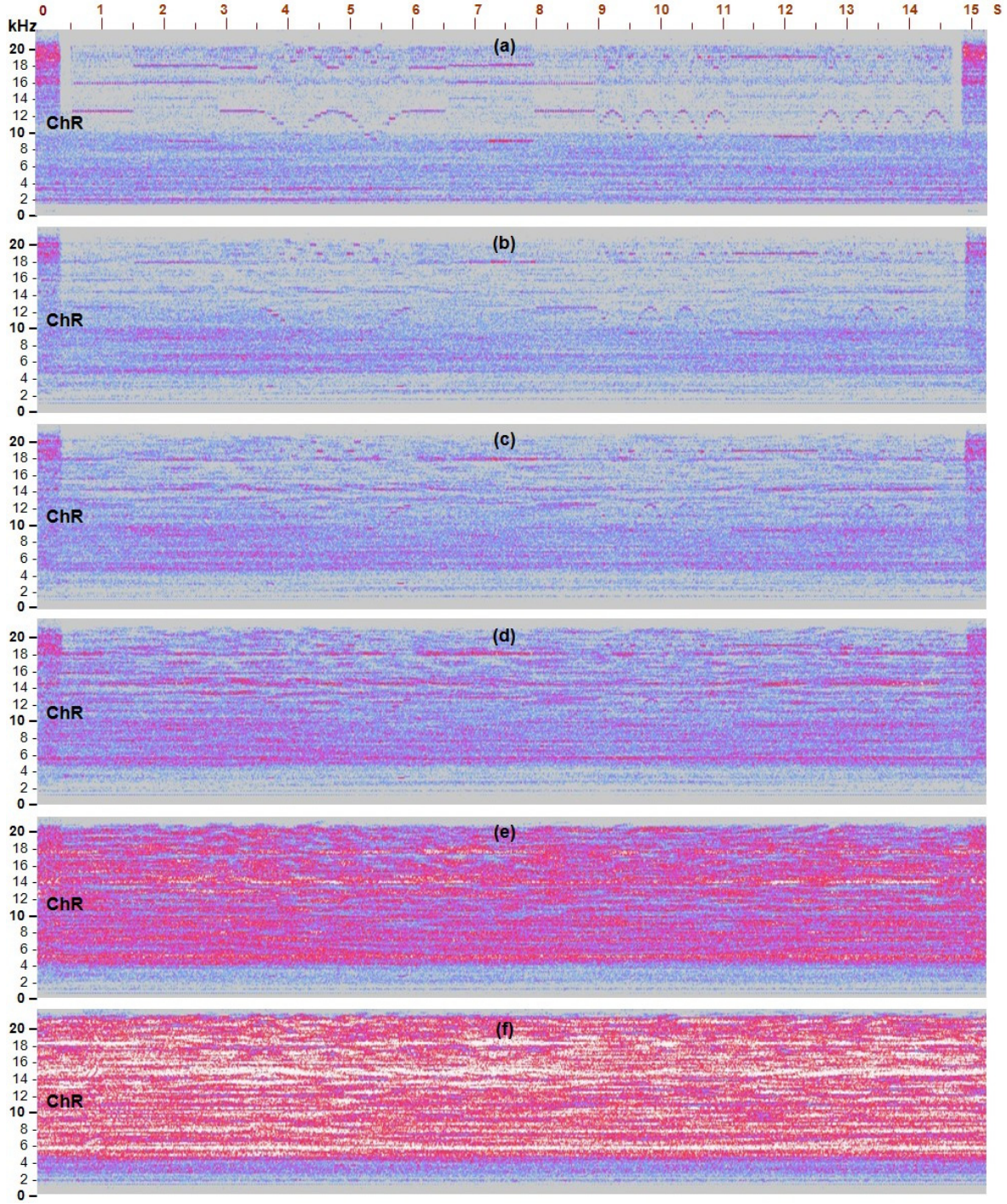


Figure 10. Spectrograms of 3D printer acoustic signals recorded during the printing of the Ghost object, masked with white noise $L_{acoustic\_noise\_White}$ at the following levels: (**a**) 0 dB (without masking), (**b**) 40 dB, (**c**) 50 dB, (**d**) 60 dB, (**e**) 70 dB, (**f**) 80 dB.

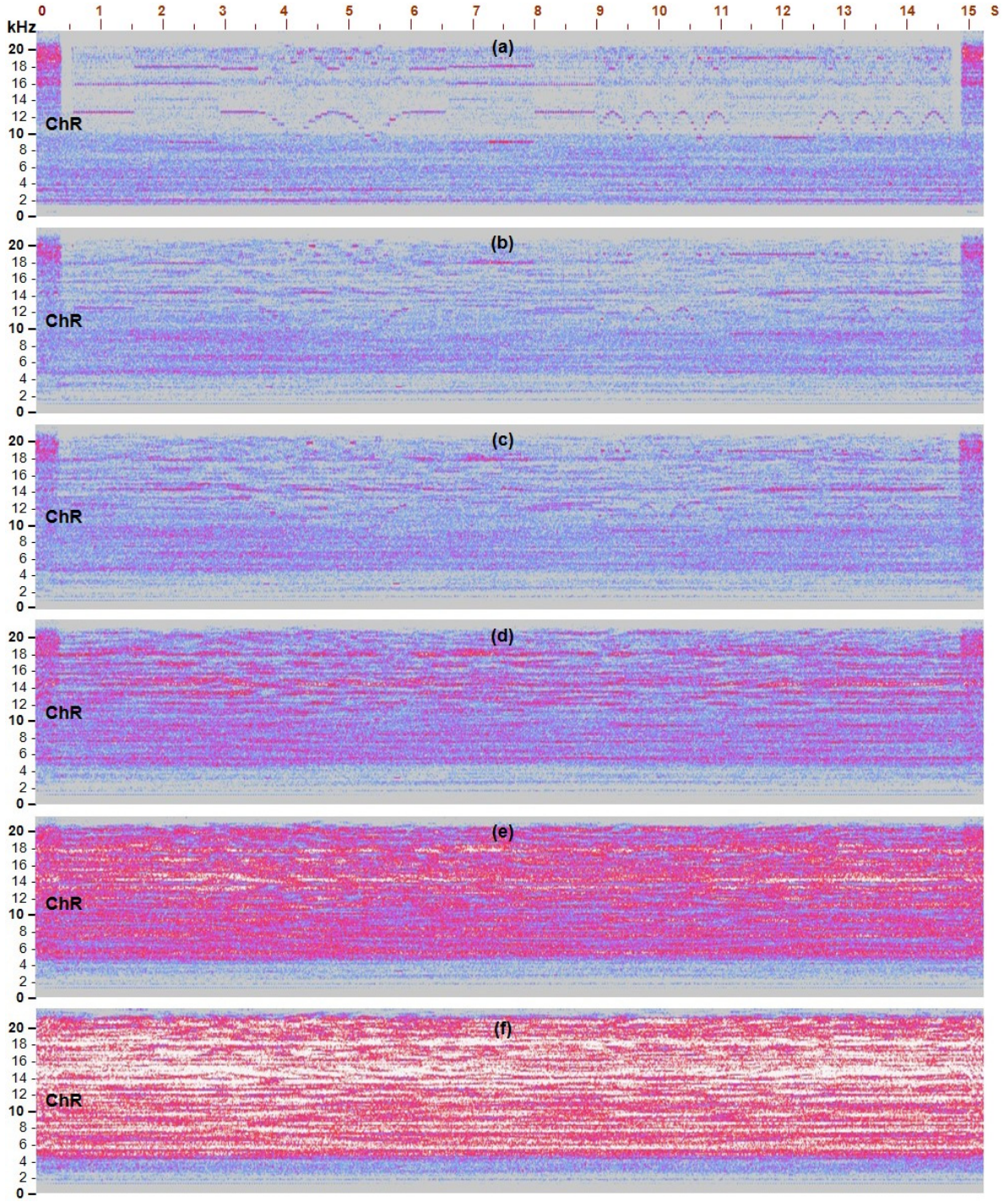


Figure 11. Spectrograms of 3D printer acoustic signals recorded during the printing of the Ghost object, masked with blue noise $L_{acoustic\_noise\_\_Blue}$ at the following levels: (**a**) 0 dB (without masking), (**b**) 40 dB, (**c**) 50 dB, (**d**) 60 dB, (**e**) 70 dB, (**f**) 80 dB.

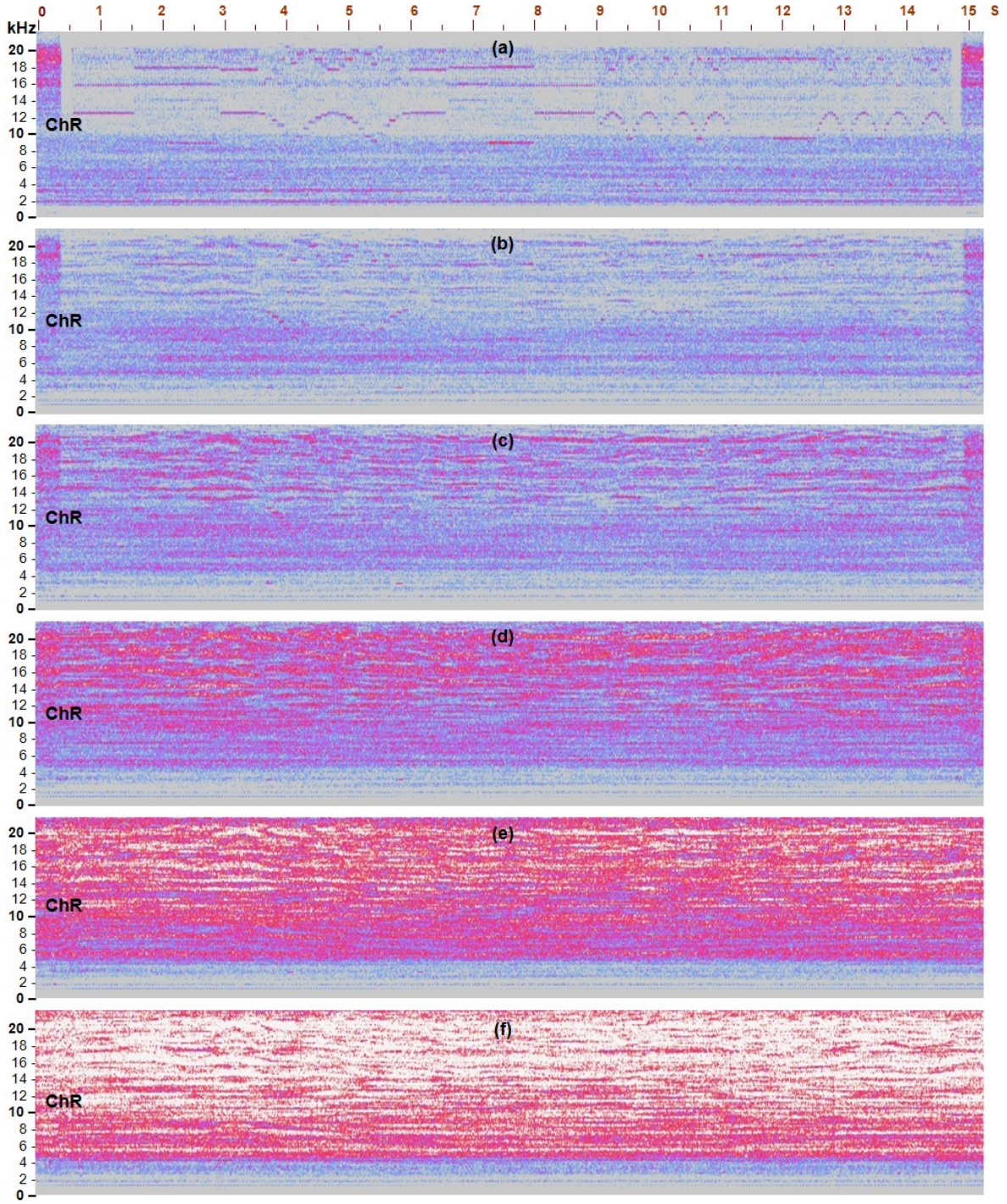


Figure 12. Spectrograms of 3D printer acoustic signals recorded during the printing of the Ghost object, masked with gray noise $L_{acoustic\_noise\_Gray}$ at the following levels: (**a**) 0 dB (without masking), (**b**) 40 dB, (**c**) 50 dB, (**d**) 60 dB, (**e**) 70 dB, (**f**) 80 dB.

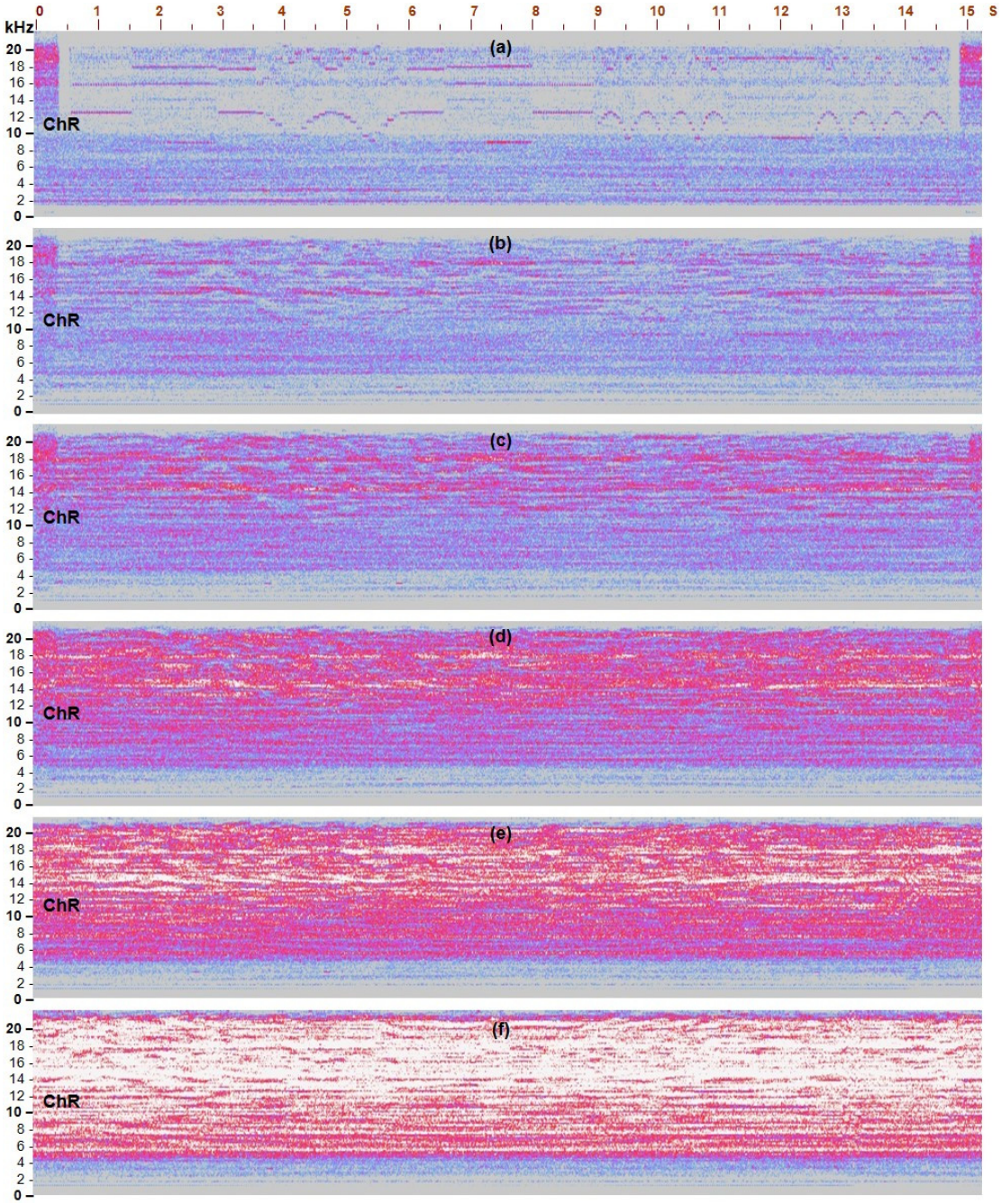


Figure 13. Spectrograms of 3D printer acoustic signals recorded during the printing of the Ghost object, masked with violet noise $L_{acoustic\_noise\_Violet}$ at the following levels: (**a**) 0 dB (without masking), (**b**) 40 dB, (**c**) 50 dB, (**d**) 60 dB, (**e**) 70 dB, (**f**) 80 dB.

In the case of blue noise with a level of $L_{acoustic\_noise\_Blue} = 60$ dB, the lines correlated with the printed object are no longer noticeable in the spectrogram. For gray noise, this situation occurs already at the noise level $L_{acoustic\_noise\_Gray}$ [dB] ≈ 50 dB.

The test result confirms that the best masking properties are observed for violet noise: at the level $L_{acoustic\_noise\_Violet} = 40$ dB, it is practically impossible to recognize individual elements of the print, and at the level $L_{acoustic\_noise\_Violet} = 60$ dB, even the head positioning phases are not visible.

3.4. Analysis of Research Results on the Effectiveness of Protecting 3D Printers against Acoustic Infiltration

3.4.1. Visual Analysis

Masking the sounds produced by a 3D printer during its operation, mainly coming from the stepper motors, print head and platform installed in it, is not too complicated. The research has shown that the desired masking effect can be achieved by creating noise at an appropriate loudness level. The masking effectiveness (visually assessed on the basis of the obtained spectrograms) is different for each type of noise: it is the highest for violet noise and the lowest for white noise—at the same noise loudness levels expressed in decibels.

A certain drawback is the need to have a sound system for the proposed solution (speakers, power amplifier, recorded noise signal player, sound level meter and cabling). The cost of such a set is not high and ranges from EUR 1000 to 1500.

Another inconvenience may be the need to have a space to locate the abovementioned elements of the set at the printer's workstation. However, both of these obstacles are incomparably less burdensome (costly) than, for example, the use of structurally complex and expensive professional sound-absorbing cabins to protect against acoustic eavesdropping.

Attention also needs to be paid to the issue of noise nuisance with levels in the range of 60–80 dB for the staff operating the printer. Although the perception of such signals is subjective and depends on the individual properties of human hearing, in most cases, the noise will be perceived as noise causing discomfort and fatigue. Therefore, personnel should stay in the printer's operating environment for no longer than a few minutes or use protective headphones or other noise attenuators.

It should be added that the perception of a noise signal depends on its type and is also a subjective feature: some people tolerate blue noise better, while others tolerate purple or gray noise with the same sound intensity level. Therefore, the choice of the type of noise and the level of its emission should be made in the actual acoustic conditions of the room in which the printer and the staff operating it are located.

To sum up, the proposed method of protecting 3D printers against acoustic infiltration when printing prototypes of secret devices is a simple and inexpensive solution to increase the level of information security. The use of appropriate noise (e.g., purple or gray) allows for better masking effects compared to other types of noise, with much lower emission levels (even by 20–30 dB).

A collective comparison of the masking properties of selected noises at the recommended emission levels of 40 dB and 50 dB is presented in Figure 14 and Figure 15, respectively (the Ghost was the printed object), and the values of the required levels of individual types of noise are included in Table 1.

Table 1. Values of the levels of individual types of noise required for effective masking of sensitive acoustic signals of the tested 3D printer.

Type of Noise	Masking Effectiveness of Printer Sounds		
	Accepted	**Good**	**Very Good**
White noise	60 dB	70 dB	80 dB
Blue noise	60 dB	70 dB	80 dB
Gray noise	50 dB	60 dB	70 dB
Violet noise	40 dB	50 dB	60 dB

3.4.2. Correlation Analysis

As part of the research on the effectiveness of masking acoustic emissions with selected types of noise, a correlation analysis was carried out between the reference signal, which is the $L_{acoustic\_printer}$ signal, and the L_{dist}, which is the reference signal disturbed by the appropriate color noise:

$$L_{dist} = L_{acoustic\_noise} + L_{acoustic\_printer}, \quad (2)$$

To assess the degree of correlation of the mentioned signals, calculated according to the equation:

$$r_{L_{acoustic\_printer},L_{dist}} = \frac{A}{B \cdot C}, \tag{3}$$

where:

$$A = \sum_{i=0}^{N-1} \left(\left(L_{acoustic\_printer}\ (i) - \overline{L_{acoustic\_printer}} \right) \cdot \left(L_{dist}(i) - \overline{L_{dist}} \right) \right), \tag{4}$$

$$B = \sum_{i=0}^{N-1} \left(L_{acoustic\_printer}\ (i) - \overline{L_{acoustic\_printer}} \right)^2, \tag{5}$$

$$C = \sum_{i=0}^{N-1} \left(L_{dist}\ (i) - \overline{L_{dist}} \right)^2, \tag{6}$$

$$\overline{L_{acoustic\_printer}} = \frac{1}{N} \sum_{i=0}^{N-1} L_{acoustic\_printer}\ (i), \tag{7}$$

$$\overline{L_{dist}} = \frac{1}{N} \sum_{i=0}^{N-1} L_{dist}\ (i), \tag{8}$$

conventional degrees of dependency between signals were assumed (Table 2).

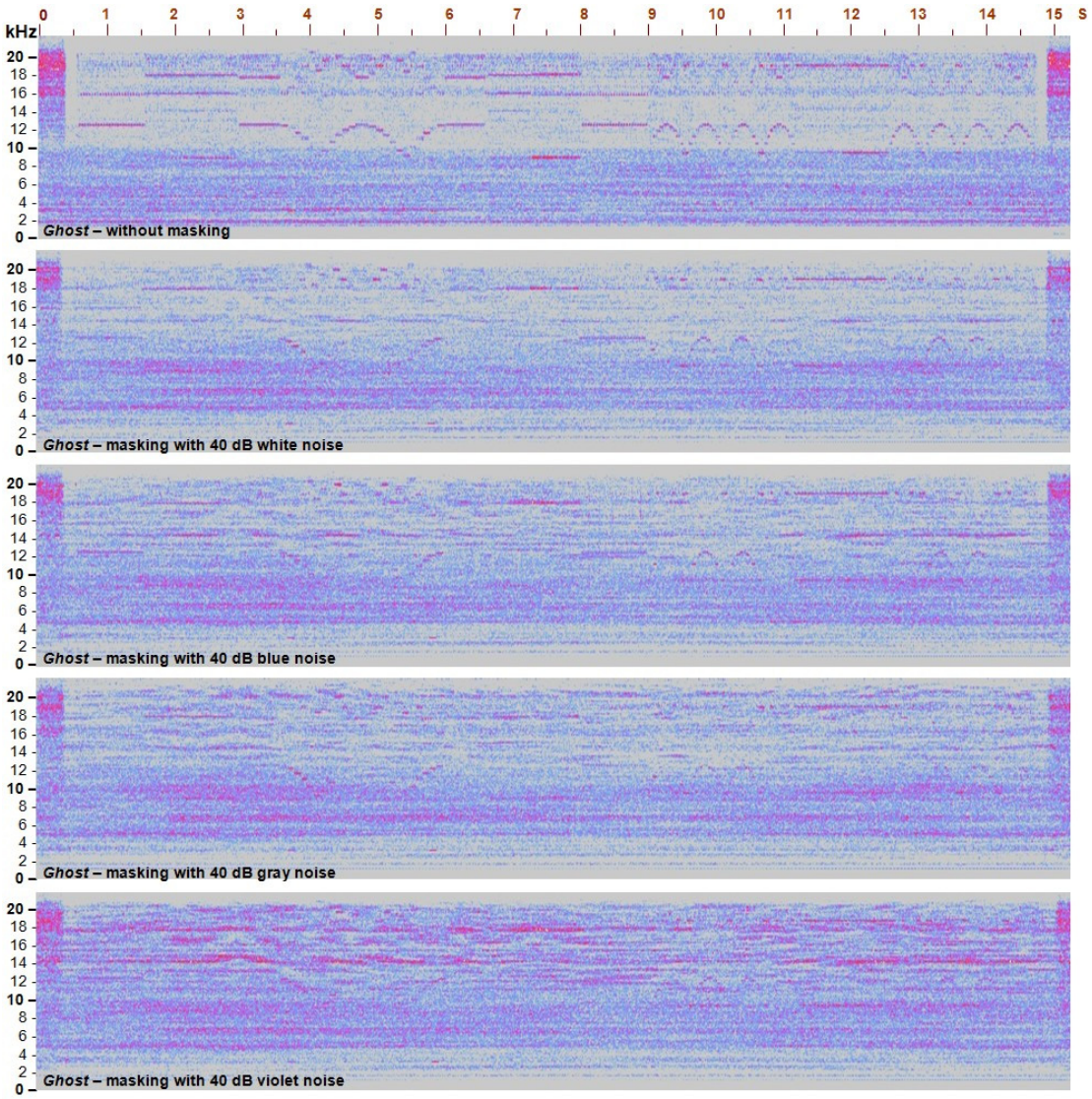


Figure 14. Comparison of noise masking properties, noise level 40 dB.

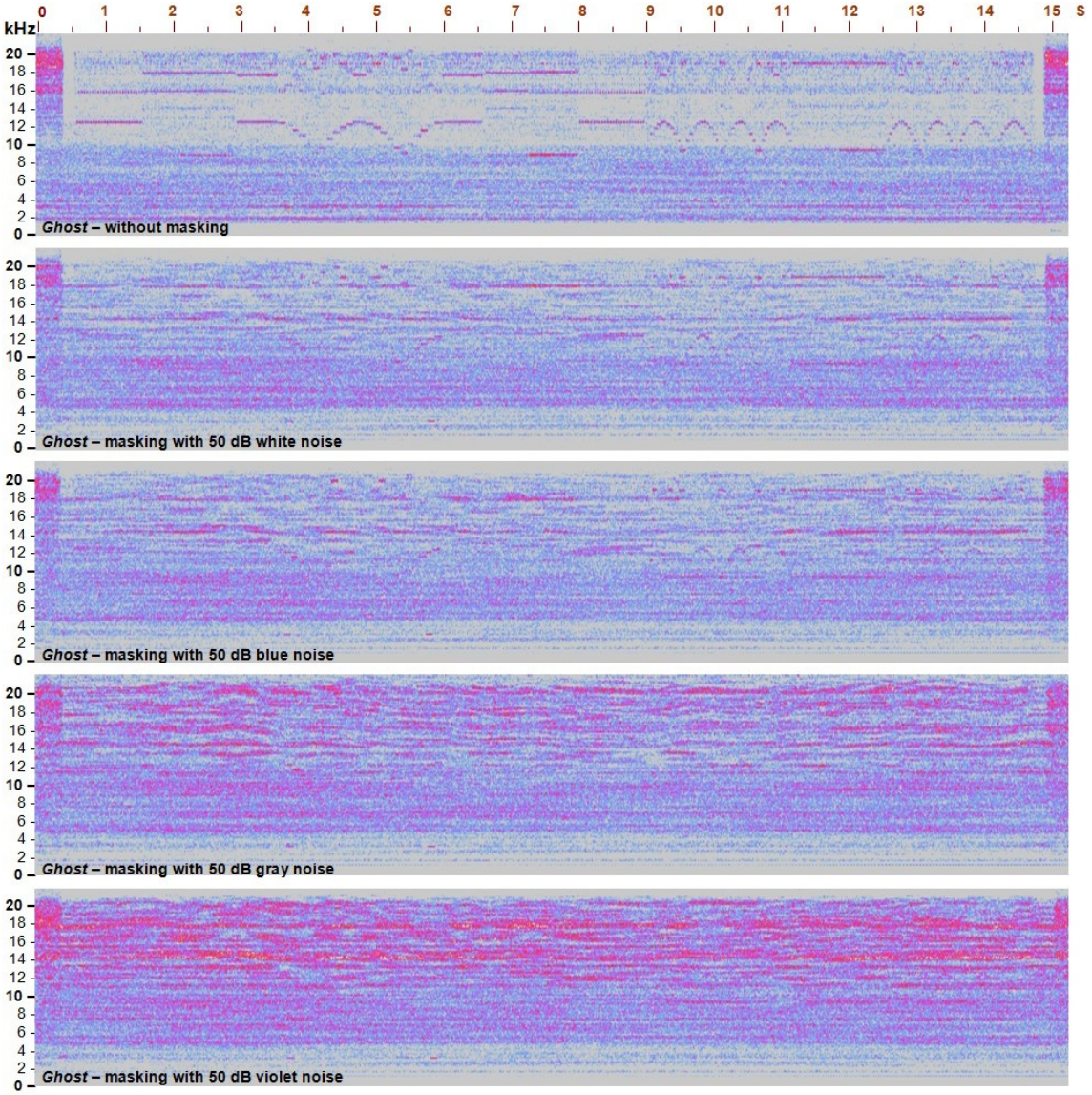


Figure 15. Comparison of noise masking properties, noise level 50 dB.

Table 2. Values of the correlation coefficient and the corresponding conventional degrees of dependence.

Values of Correlation Coefficient	Conventional Degrees of Dependence
$R < 0.2$	lack relationship
$0.2 \leq R < 0.4$	weak relationship
$0.4 \leq R < 0.7$	moderate relationship
$0.7 \leq R < 0.9$	strong relationship
$R \geq 0.9$	very strong relationship

The analysis of spectrograms obtained without noise shows that the frequency range from 0 to approximately 9 kHz is the range in which there are no signals useful for conducting the acoustic infiltration process. However, they may negatively influence (inflate) the obtained values of the correlation coefficient. Hence, the correlation analysis was preceded by filtering the signal with a high-pass filter with a cut-off frequency of $f_c = 9$ kHz and a slope of 48 dB per octave. An example result of applying filtering is shown in Figure 16, showing spectrograms before and after the filtering of the acoustic signal $L_{acoustic\_printer}$ without noise and with blue noise $L_{acoustic\_noise\_Blue}$ at a level of 40 dB.

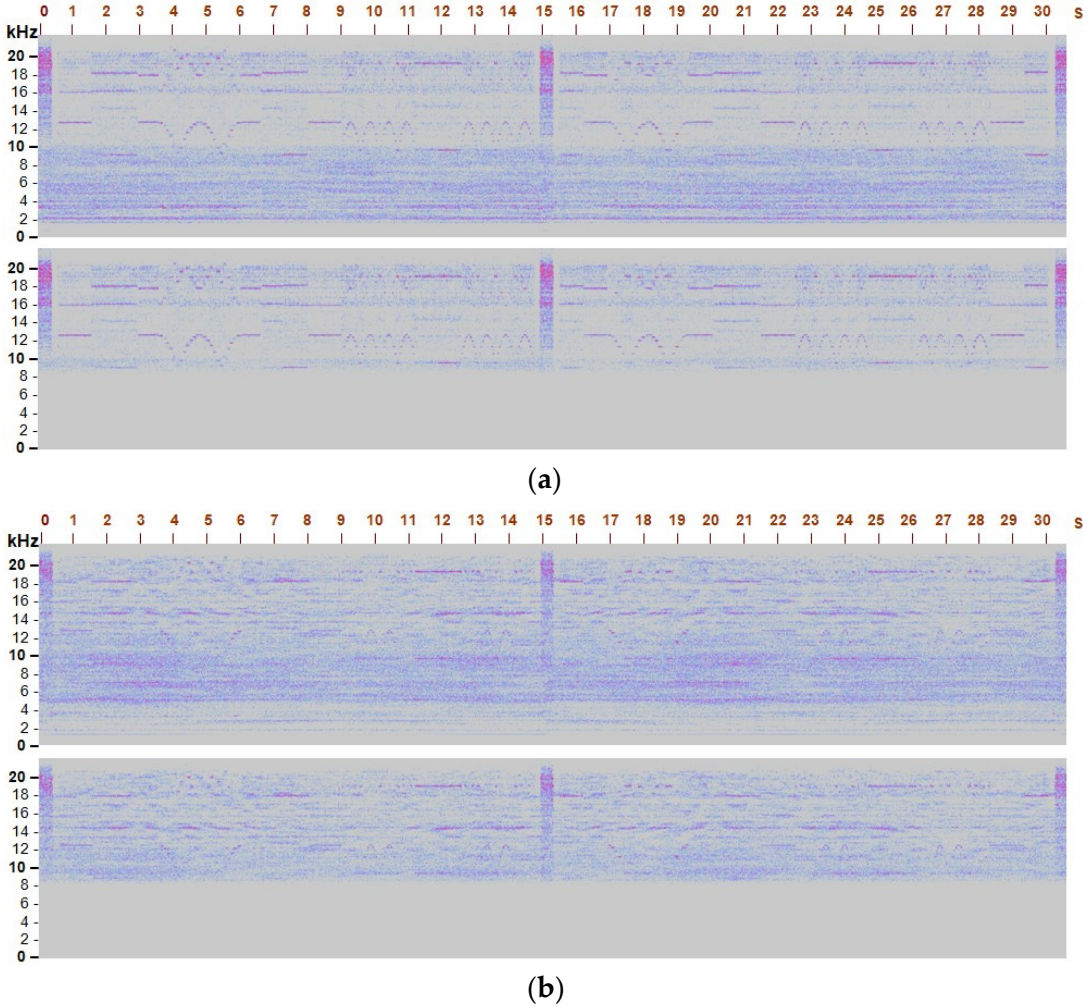


Figure 16. Spectrograms for signals (**a**) unnoised before and after filtering and (**b**) noised with 40 dB blue noise before and after filtering.

Detailed calculations of the correlation coefficient $r_{L_{acoustic\_printer}, L_{dist}}$ were performed for white, violet, gray and blue noise with $L_{acoustic\_noise}$ levels of 40 dB, 50 dB, 60 dB, 70 dB and 80 dB. As a result of the calculations for the conditions described above, the values of the correlation coefficient presented in Figure 17 and Table 3 were obtained.

The numerical values of the correlation coefficient $r_{L_{acoustic\_printer}, L_{dist}}$ confirm the results of visual analysis, for which the most effective noises in the process of counteracting acoustic infiltration of a 3D printer are purple noise and gray noise. Nevertheless, the values of the correlation coefficient $r_{L_{acoustic\_printer}, L_{dist}}$ for violet noise decrease faster as the noise level increases and reach the value of 0.1576 and the value of 0.1790 for gray noise, with a noise level of 60 dB.

It should be noted that the acoustic frequencies useful in the infiltration process range from approximately 9 kHz to approximately 19 kHz. The power spectral density $S(f)$ distribution for violet and gray noise covers these frequencies most effectively. Blue noise has similar characteristics $S(f)$, but for which the values of the correlation coefficient $r_{L_{acoustic\_printer}, L_{dist}}$ decrease more slowly as the noise level increases. The worst performance is white noise with a constant distribution of power spectral density $S(f)$.

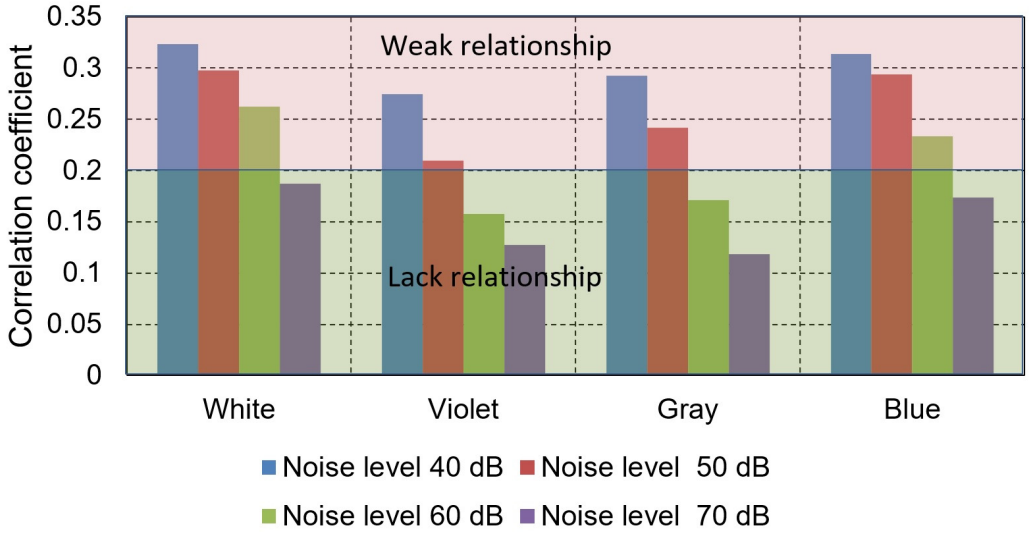


Figure 17. Maximum values of the correlation coefficient $r_{L_{acoustic\_printer}\_L_{dist}}$ calculated for different levels $L_{acoustic\_noise}$ of color noise.

Table 3. Maximum values of the correlation coefficient $r_{L_{acoustic\_printer},L_{dist}}$ calculated for different levels of $L_{acoustic\_noise}$ of color noise.

Noise Level [dB]	Type of Noise			
	White	**Violet**	**Gray**	**Blue**
40	0.3236 *	0.2748 *	0.2925 *	0.3140 *
50	0.2977 *	0.2095 *	0.2416 *	0.2938 *
60	0.2626 *	0.1576 **	0.1790 **	0.2334 *
70	0.1875 **	0.1272 **	0.1184 **	0.1736 **
80	≈0.0000 **	≈0.0000 **	≈0.0000 **	≈0.0000 **

*—weak relationship. **—lack relationship.

4. Conclusions

In the article, an analysis of acoustic emissions produced by a 3D printer during its operation was shown and the effectiveness of masking acoustic signals produced by a 3D printer with noise was assessed. Based on the obtained spectrograms, it was found that the levels of the abovementioned emissions do not depend on the complexity of the printed objects.

The correlation analysis of the noisy (standard) signal and the signal masked with various noises with levels ranging from 40 dB to 80 dB confirmed the previously performed visual analysis of the obtained spectrograms. Due to the fact that signals in the 0–9 kHz band do not contain important information about the shape of the printed object, the noisy signal was filtered using a high-pass filter with a cut-off frequency of $f_c = 9$ kHz and a slope of 48 dB per octave. The intuitive and obvious conclusion that the effectiveness of masking depends on the level of masking noise was supplemented by the statement that the spectral characteristics of the noise used also play an important role.

The method of the practical implementation of the security measures in question is presented in Section 3. The masking properties of three selected colored noises (gray, blue and purple) are compared with those of white noise. The intensity levels at which the acoustic safety of the printer can be ensured without endangering the hearing of the personnel operating the device have been determined.

Based on the obtained results, it should be concluded that purple noise is best for applications preventing the acoustic infiltration of a 3D printer. Already at a level of 40 dB, it can acceptably prevent the acoustic infiltration of the tested device, which produces sounds with an intensity of 55–57 dB during printing. It should be emphasized that the

power spectral density of these sounds is the highest in the frequency range 2–9 kHz, where the printer's acoustic emissions do not contain significant information from the point of view of its susceptibility.

It should be noted that the types and levels of noise used to mask acoustic signals do not slow down the printing process itself, as these parameters do not affect the operation of the printer. It can only be assumed that in the case of extremely high noise levels (of the order of at least one hundred or several dozen dB), printer vibrations could occur, which would potentially affect the print quality. A certain drawback of the proposed method is the fact that it is not cost-free—it requires certain financial outlays for the purchase of electroacoustic devices listed in Section 2.2. However, the costs of the presented solution are small compared to the benefits resulting from ensuring the security of information about printed objects.

Another inconvenience is the need to assess the effectiveness of the solution in a specific manufacturing environment by recording acoustic signals generated during a test print of an object: without masking and with masking with noise of the recommended type and intensity. To carry out this assessment, basic knowledge in the field of digital signal processing and physical phenomena occurring in the subject area of research is necessary.

Tests on the effectiveness of masking acoustic signals using color noise were carried out for the Zortrax M200 Plus 3D printer. The extensive experience of the authors of the article in the area of protection of information against electromagnetic penetration allows for the conclusion that the use of a given solution for one type of device does not necessarily guarantee success in suppressing sensitive electromagnetic emissions of another type of such device. This is related to both the design of the device and its hardware configuration. A similar phenomenon can be observed in the case of 3D printers. The possibility of a wider use of the method presented in this article must therefore be verified for other types of 3D printers. This is related to the possible occurrence of acoustic signals for such printers in the range of other frequencies. This approach is necessary to find a universal solution (for as many different types of printers as possible) to counteract non-invasive information acquisition using acoustic infiltration.

Further works are planned for the Full Color 3D da Vinci Series printer. This is a more mechanically advanced printer that uses color printing. Therefore, there may be additional sources of unwanted acoustic signals correlated with the shape of printed objects.

Author Contributions: Conceptualization, A.S. and I.K.; methodology, A.S.; software, A.S. and I.K.; validation, A.S. and I.K.; formal analysis, A.S.; investigation, A.S. and I.K.; data curation, A.S.; writing—original draft preparation, A.S.; writing—review and editing, A.S. and I.K.; visualization, A.S.; supervision, A.S. All authors have read and agreed to the published version of the manuscript.

Funding: This research received no external funding.

Data Availability Statement: Data are contained within the article.

Conflicts of Interest: The authors declare no conflict of interest.

References

1. Jiang, Q.; Liu, Q.; Wu, S.; Zheng, H.; Sun, W. Modification effect of nanosilica and polypropylene fiber for extrusion-based 3D printing concrete: Printability and mechanical anisotropy. *Addit. Manuf.* **2022**, *56*, 102944. [CrossRef]
2. Liu, Q.; Jiang, Q.; Huang, M.; Xin, J.; Chen, P.; Wu, S. Modifying effect of anionic polyacrylamide dose for cement-based 3DP materials: Printability and mechanical performance tests. *Constr. Build. Mater.* **2022**, *330*, 127156. [CrossRef]
3. Żukowska, M.; Rad, M.A.; Górski, F. Additive Manufacturing of 3D Anatomical Models—Review of Processes, Materials and Applications. *Materials* **2023**, *16*, 880. [CrossRef] [PubMed]
4. Ribeiro, J.; Filgueiras, H.; Sodré Junior, A.; Beltrán-Mejía, F.; Mejía-Salazar, J. 3D-Printed Quasi-Cylindrical Bragg Reflector to Boost the Gain and Directivity of cm- and mm-Wave Antennas. *Sensors* **2021**, *21*, 8014. [CrossRef]
5. Zeng, C.; Faaborg, M.W.; Sherif, A.; Falk, M.J.; Hajian, R.; Xiao, M.; Hartig, K.; Bar-Sinai, Y.; Brenner, M.P.; Manoharan, V.N. 3D-printed machines that manipulate microscopic objects using capillary forces. *Nature* **2022**, *611*, 68–73. [CrossRef]
6. Islam, M.N.; Tu, Y.; Hossen, M.I.; Guo, S.; Hei, X. A Survey on Limitation, Security and Privacy Issues on Additive Manufacturing. *arXiv* **2021**, arXiv:2103.06400.

7. Yampolskiy, M.; King, W.E.; Gatlin, J.; Belikovetsky, S.; Brown, A.; Skjellum, A.; Elovici, Y. Security of Additive Manufacturing: Attack Taxonomy and Survey. *Addit. Manuf.* **2018**, *21*, 431–457. [CrossRef]
8. Al Faruque, M.A.; Chhetri, S.R.; Canedo, A.; Wan, J. Acoustic Side-Channel Attacks on Additive Manufacturing Systems. In Proceedings of the IEEE/ACM 7th International Conference on Cyber-Physical Systems (ICCPS), Vienna, Austria, 11–14 April 2016. [CrossRef]
9. Al Faruque, M.A.; Chhetri, S.R. Side Channels of Cyber-Physical Systems: Case Study in Additive Manufacturing. *IEEE Des. &Test* **2017**, *34*, 18–25. [CrossRef]
10. Kubiak, I.; Przybysz, A.; Stańczak, A. Usefulness of Acoustic Sounds from 3D Printers in an Eavesdropping Process and Reconstruction of Printed Shapes. *Electronics* **2020**, *9*, 297. [CrossRef]
11. Stańczak, A.; Kubiak, I.; Przybysz, A.; Witenberg, A. The possibility to recreate the shapes of objects on the basis of printer vibration in the additive printing process. *Appl. Sci.* **2021**, *11*, 5305. [CrossRef]
12. Gatlin, J.; Belikovetsky, S.; Elovici, Y.; Skjellum, A.; Lubell, J.; Witherell, P.; Yampolskiy, M. Encryption is Futile: Reconstructing 3D-Printed Models Using the Power Side-Channel, RAID '21. In Proceedings of the 24th International Symposium on Research in Attacks, Intrusions and Defenses, San Sebastian, Spain, 6–8 October 2021. [CrossRef]
13. Poggi, D. Simulating and Interpreting EM Side-Channel Attacks at Chip Level Prior to Fabrication, Electromagnetism, Université de Montpellier, 2022, English, ffNNT: 2022UMONS006. Available online: https://theses.hal.science/tel-03851237/ (accessed on 14 November 2022).
14. Chhetri, S.R.; Faezi, S.; Faruque, M.A. Fix the Leak! An Information Leakage Aware Secured Cyber-Physical Manufacturing System. In Proceedings of the Design, Automation & Test in Europe Conference Exhibition (DATE), Lausanne, Switzerland, 27–31 March 2017.
15. Song, C.; Lin, F.; Ba, Z.; Ren, K.; Zhou, C.; Xu, W. My Smartphone Knows What You Print: Exploring Smartphone-Based Side-Channel Attacks against 3d Printers. In Proceedings of the 2016 ACM SIGSAC Conference on Computer and Communications Security, CCS '16, Vienna, Austria, 24–28 October 2016. [CrossRef]
16. Knechtel, J.; Sinanoglu, O. On Mitigation of Side-Channel Attacks in 3D ICs: Decorrelating Thermal Patterns from Power and Activity. In Proceedings of the 54th ACM/EDAC/IEEE Design Automation Conference (DAC), Austin, TX, USA, 18–22 June 2017. [CrossRef]
17. Al Faruque, M.A.; Chhetri, S.R.; Faezi, S.; Canedo, A. Forensics of Thermal Side-Channel in Additive Manufacturing Systems. *Univ. Calif. Irvine* **2016**, *12*, 176.
18. Mahesh, P.; Tiwari, A.; Jin, C.; Kumar, P.R.; Reddy, A.L.; Bukkapatanam, S.T.; Gupta, N.; Karri, R. A Survey of Cybersecurity of Digital Manufacturing. *Proc. IEEE* **2021**, *109*, 495–516. [CrossRef]
19. Mativo, T.; Fritz, C.; Fidan, I. Cyber acoustic analysis of additively manufactured objects. *Int. J. Adv. Manuf. Technol.* **2018**, *96*, 581–586. [CrossRef]
20. Macovei, A.; Boitan, A.; Trip, B.; Butnariu, V.; Roşu, G.; Halunga, S. Detection of Electromagnetic Emissions Transmitted on the Power Line through Electrical Conduction. In Proceedings of the International Conference on Applied and Theoretical Electricity (ICATE), Craiova, Romania, 4–6 October 2018. [CrossRef]
21. Trip, B.; Butnariu, V.; Velicu, V.; Halunga, S.; Boitan, A. Analysis of the Compromising Audio Signal from the Emission Security Perspective. In Proceedings of the 13th International Conference on Communications (COMM), Bucharest, Romania, 18–20 June 2020. [CrossRef]
22. Tajima, K.; Ishikawa, R.; Mori, T.; Suzuki, Y.; Takaya, K. A Study on Risk Evaluation of Countermeasure Technique for Preventing Electromagnetic Information Leakage from ITE. In Proceedings of the International Symposium on Electromagnetic Compatibility EMC Europe, Angers, France, 4–7 September 2017.
23. Yu, S.Y.; Malawade, A.V.; Chhetri, S.R.; Al Faruque, M.A. Sabotage Attack Detection for Additive Manufacturing Systems. *IEEE Access* **2020**, *8*, 27218–27231. [CrossRef]
24. Backes, M.; Dürmuth, M.; Gerling, S.; Pinkal, M.; Sporleder, C. Acoustic Side-Channel Attacks on Printers. Available online: eecs.umich.edu (accessed on 10 March 2015).
25. Zortrax M200 Plus 3D Printer. Available online: https://www.machines-3d.com/en/zortrax-m200-plus-3d-printer-xml-351_906_384-2327.html (accessed on 1 May 2018).
26. Related Manuals for Zortrax M200 Plus. Available online: https://www.manualslib.com/manual/1476218/Zortrax-M200-Plus.html (accessed on 1 May 2018).
27. Everything about Stepper Motors—Construction, Principle of Operation, Application Botland—Robotic Shop. Available online: https://botland.store/content/220-wszystko-o-silnikach-krokowych (accessed on 5 May 2014).
28. Graves, L.M.; Lubell, J.; King, W.; Yampolskiy, M. Characteristic aspects of additive manufacturing security from security awareness perspectives. *IEEE Access* **2019**, *7*, 103833–103853. [CrossRef] [PubMed]
29. Do, Q.; Martini, B.; Choo, K.-K.R. A Data Exfiltration and Remote Exploitation Attack on Consumer 3D Printers. *IEEE Trans. Inf. Forensics Secur.* **2016**, *11*, 2174–2186. [CrossRef]

30. Gatlin, J.; Belikovetsky, S.; Moore, S.B.; Solewicz, Y.; Elovici, Y.; Yampolskiy, M. Detecting Sabotage Attacks in Additive Manufacturing Using Actuator Power Signatures. *IEEE Access* **2019**, *7*, 133421–133432. [CrossRef]
31. Stańczak, A.; Kubiak, I.; Przybysz, A. Masking the Acoustic Signals Generated by 3D Printers using Variety of Noise Types. In Proceedings of the 39th IBIMA Conference, Granada, Spain, 30–31 May 2022.

Disclaimer/Publisher's Note: The statements, opinions and data contained in all publications are solely those of the individual author(s) and contributor(s) and not of MDPI and/or the editor(s). MDPI and/or the editor(s) disclaim responsibility for any injury to people or property resulting from any ideas, methods, instructions or products referred to in the content.